ELSEVIER

Polymer 40 (1999) 2829–2836

polymer

A TEM study on polyoxymethylene edge-on lamellae crystallized epitaxially on alkali halides

Masahiro Fujita, Masaki Tsuji*, Shinzo Kohjiya

Laboratory of Polymer Condensed States, Division of States and Structures III, Institute for Chemical Research, Kyoto University, Uji, Kyoto-fu 611-0011, Japan

Received 27 March 1998; accepted 18 June 1998

Abstract

Rodlike crystals of polyoxymethylene (POM) were isothermally grown on the (001) face of NaCl or KCl from 0.1 wt% solutions (solvent: nitrobenzene, acetophenone, benzyl alcohol, *m*-cresol). Transmission electron microscopic observation in bright and dark-field imaging modes and selected-area electron diffraction analysis successfully evidenced that POM chain stems in the rodlike crystals are set parallel to the substrate surface and also perpendicular to the rod axis. That is to say, each rodlike crystal was well identified as an edge-on lamella. Further, it was confirmed that the width of bright striations in the dark-field images, which correspond to the crystalline-core thickness of the edge-on lamella, depended on the crystallization temperature (T_c) and increased with increasing lamellar thickness. The crystalline-core thickness was, however, inevitably smaller than the corresponding lamellar thickness for any T_c. It was accordingly concluded that the POM edge-on lamella has a surface layer (20%–25% of the lamellar thickness) containing folds on each side of the lamella, the layer is presumed to be composed of adjacent re-entrant folds which have some fluctuation in contour length and resultant fluctuation in conformation.

Keywords: Polyoxymethylene; Epitaxy; Edge-on lamella

1. Introduction

Epitaxy of various polymers on alkali halides was extensively studied, mainly by transmission electron microscopy (TEM) and the works on polymer epitaxy were surveyed in several review articles [1,2]. Most of the examined polymers are flexible linear polymers, such as polyethylene (PE). For example, PE is grown on the (001) face of an alkali halide and the resultant morphology is characterized by fibrous or rodlike crystals orientated in the [110] and [$\bar{1}$10] directions (namely, the ⟨110⟩ directions) of the alkali halide. From the corresponding electron diffraction pattern, it is interpreted that the rodlike crystal of PE is an edge-on lamella in which the chain-stem axis is parallel to the substrate surface and perpendicular to the long axis of the rodlike crystal. Epitaxial crystallization of polyoxymethylene (POM) on various alkali halides has also been studied so much [1–11]. Similarly to the epitaxy of PE, the typical morphology of POM on an alkali halide observed by TEM appears to be rodlike crystals orientated in the ⟨110⟩ directions of the substrate [4–6,8,9,11], though single-crystal-like flat-on platelets were also occasionally observed [3–5,8,9]. It was evidenced by electron diffraction that the molecular stems in such rodlike crystals lie parallel to the (001) face of the substrate and also orientate in the ⟨110⟩ directions of the substrate [5,8,9]. The energy calculation well supports this orientation of the POM stems on the substrate [7,10].

Although there had been published rather many morphological studies on the epitaxy of POM on the alkali halides, no conclusive experimental evidences were reported on the orientation of molecular stems in the rodlike crystals. Recently, it was proposed that the molecular stems in the rodlike crystal of POM grown epitaxially on NaCl might be set parallel to the long axis of the rod with a triangular cross-section [11]. Before this proposal, it had been expected that the stems in the rod should be packed normal to its long axis, that is, each of the rodlike crystals of POM had been regarded as an 'edge-on' lamella [9]. In our previous work [12], we elucidated, by dark-field TEM observation and selected-area electron diffraction (SAED) experiment, that the molecular stems of POM in the rodlike crystal grown on NaCl are set perpendicular to the long axis of the rod. In the dark-field images, the crystalline core of each edge-on lamella was visualized as a bright striation. In the case of

* Corresponding author. E-mail: tsujimas@scl.kyoto-u.ac.jp

0032-3861/99/$ - see front matter
PII: S0032-3861(98)00495-9

Table 1
Crystallization condition

Solvent	T_d^0 [17] (°C)	T_c (°C)	$1/\Delta T \times 10^3$ (K^{-1})
m-cresol	132.7	85	21.0
Benzyl alcohol	153.2	115	26.2
		125	35.5
Acetophenone	161.3	125	27.5
		135	38.0
Nitrobenzene	—	150	—

T_d^0: equilibrium dissolution temperature; T_c: crystallization temperature; $\Delta T \equiv T_d^0 - T_c$: degree of supercooling.

the edge-on lamellae of PE, it was reported, from comparative studies on solution-grown lamellar crystals of PE and some cycloparaffins, that in PE the width of such a bright striation, namely the crystalline-core thickness, was smaller than the lamellar thickness and was increased with increasing crystallization temperature [13]. It is, thus, expected that this conclusion might also be applicable to POM.

In the present work, the morphologies of the rodlike crystals of POM grown on the alkali halides were observed by TEM in bright and dark-field imaging modes and the dependence of the crystalline-core thickness on the crystallization temperature was discussed by comparing with that for PE.

2. Experimental

2.1. Sample preparation

The procedure of sample preparation was similar to that in our previous work [12]. POM (TENAC 5010, Asahi Chemical Industry Co. Ltd) with a molecular weight of about 40 000 was utilized in this study without further purification. The substrates used here were NaCl and KCl, the (001) faces of which were freshly cleaved just before epitaxial crystallization, because it had been reported that only the hexagonal form of POM is to grow on both of them [8]. Solvents used here were nitrobenzene, acetophenone, benzyl alcohol and *m*-cresol. At desired crystallization temperatures (T_c) shown in Table 1, the epitaxial crystallization was performed isothermally in an 0.1 wt% solution of POM under a nitrogen atmosphere. The precision of temperature regulation was at worst within $\pm$ 1 degree for a given T_c. The crystallization time was 60 s in all cases.

The specimens on NaCl and KCl were shadowed under vacuum with Pt–Pd for morphological observation and thereafter coated with vapour-deposited carbon (C) under vacuum. For dark-field imaging, however, the specimens on the substrates were coated and reinforced only with C. Substrates with the specimens were then floated on the water surface with the specimen side facing up and the floating specimens were picked up on Cu grids for TEM. The shadowing angle was $\tan^{-1}(1/4)$ and the shadowing direction was parallel to the [100] direction of the substrates. For calibrating the camera length in SAED experiments, some of the specimens were shadowed with Au instead of Pt–Pd.

2.2. Transmission electron microscopy

TEM was performed with a JEOL JEM-200CS operated at 160 or 200 kV. For SAED and dark-field imaging experiments, a specimen-rotating holder (JEOL EM-SRH10) was utilized. Bright-field images were recorded on Fuji FG films to obtain higher contrast and SAED patterns and dark-field images were recorded on more sensitive films (Kodak SO-163 or Mitsubishi MEM) [14]. All the exposed films were developed with Mitsubishi Gekkol (full strength) at 20°C for 5 min.

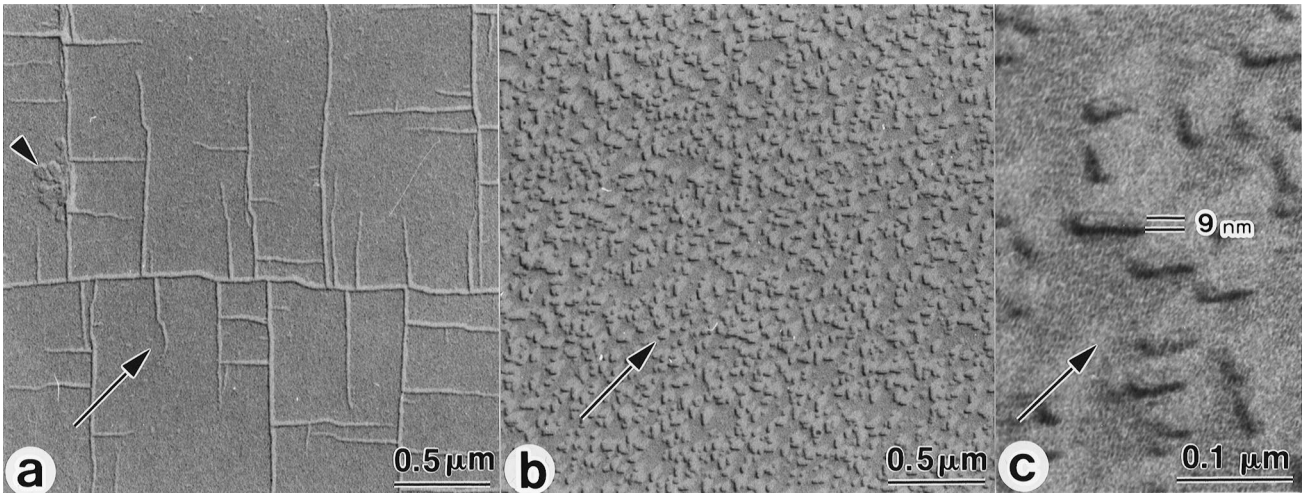

Fig. 1. Rodlike crystals of POM grown isothermally from 0.1 wt% solutions. (a) On the NaCl (001) face in nitrobenzene at 150°C; (b) on the KCl (001) face in acetophenone at 125°C; and (c) highly enlarged from (b). The arrow in each figure indicates the [100] direction of the substrate and the specimen was shadowed with Pt–Pd in this direction. The rodlike crystals are orientated in two directions perpendicular to each other.

3. Results and discussion

3.1. Morphological observations

Fig. 1a shows the typical morphology of the rodlike crystals of POM grown epitaxially on the (001) face of NaCl at 150°C in nitrobenzene and Fig. 1b and c show that on the (001) face of KCl at 125°C in acetophenone. In every figure, the arrow indicates the shadowing direction, namely the [100] direction of the substrate. By taking into account the shadowing direction, it is, thus, concluded that the rodlike crystals orientate in the ⟨110⟩ directions of the substrate, perpendicular to each other. When NaCl was used as a substrate, flat-on crystals of POM were occasionally observed [4,5,8,9,12] and, for example, such a flat-on crystal is indicated with the arrowhead in Fig. 1a. It can be seen that the crystals on KCl were grown much more densely than those on NaCl. As will be discussed below, the crystal form of the rodlike crystals of POM grown on NaCl and KCl is determined to be hexagonal (9/5 helix: $a = 0.447$ nm, c (chain axis) $= 1.739$ nm) [15]. According to Rickert and Baer [8], this hexagonal crystal lattice is more stable than the orthorhombic one (2/1 helix: $a = 0.477$ nm, $b = 0.765$ nm, c (chain axis) $= 0.356$ nm) [16] and the lattice mismatch, $|\Delta|$, between the intermolecular periodicity in the (100) plane of hexagonal POM (namely, cell constant; $a = 0.447$ nm) and the (110) lattice spacing of KCl on its (001) face is smaller than that for NaCl (see Table 2: the smaller $|\Delta|$ predicts the better lattice matching). Actually, KCl has a nearly perfect match with the hexagonal crystal lattice of POM than other alkali halides [8] and it is concluded that much more nucleation events occurred for POM on KCl as demonstrated in Fig. 1b. On the other hand, nucleation took place less frequently on NaCl and accordingly, most of the resulting rodlike crystals could grow much longer, as observed in Fig. 1a which resembles an aerial photograph of the road network in the countryside. Table 2 shows the degree of lattice matching between POM and some alkali halides (all the calculations were done on the basis of the lattice constants at room temperature). In this table, KI and KBr are also listed for comparison. As for the hexagonal form of POM whose (100) plane is expected to be in contact with the substrate [the (100) contact plane], the value of $|\Delta|$ for KBr is much smaller than that for NaCl. On KBr, however, the orthorhombic form will grow together with the hexagonal one, as on KI and RbBr [8]. Therefore, neither KBr nor KI were utilized in this report. Though the value of $|\Delta|$ for KCl and the (110) contact plane of orthorhombic POM and that for NaCl and the (100) contact plane of orthorhombic POM were calculated to be rather small, it was confirmed in our SAED patterns that only the hexagonal POM was grown on KCl and NaCl, as will be demonstrated later.

It was not easy to measure correctly the width of rodlike crystals in Fig. 1a and b. Occasionally, however, we could do so for some crystals which gave adequate mass-thickness contrast in these figures. Fig. 1c is the highly enlarged photograph from a part of Fig. 1b. One side of the crystals is enhanced in contrast by Pt–Pd shadowing. The rectangular crystals can be recognized in Fig. 1c. In this case, the average width of the rodlike crystals is estimated at 9.1 nm (± 1.7 nm: standard deviation).

Fig. 2 shows the SAED pattern taken from the rodlike crystals of POM grown epitaxially on the KCl (001) face at 125°C in acetophenone. In this figure, all the reflection spots were well indexed with the unit cell constants of the hexagonal POM with the aid of reflection rings from Au. Consequently, two *hhl* net-patterns of the hexagonal lattice, perpendicular to each other, are recognized. Therefore, it can be concluded that the chain axis orientates in either [110] or [$\bar{1}$10] direction of KCl and the contact plane of the rodlike crystal is the (100) plane of hexagonal POM, as on NaCl [12]. Only from these results, however, it is not possible to clarify the direction of chain axis in each rodlike crystal. In the rodlike crystal grown epitaxially on NaCl, it was proposed in 1990 that the direction of chain axis might be set parallel to the long axis of the rod [11]. Before this proposal, it had been expected that the rodlike

Table 2
Lattice mismatching of polyoxymethylene with alkali halides

Crystal system: contact plane/ϵ[a] (nm)	$\|\Delta\|$[a] (lattice mismatch)			
	KCl	NaCl	KI	KBr
Hexgonal:				
(100)/0.447	0.45	12	11	4.2
Orthorhombic:				
(110)/0.451	1.3	13	9.8	3.4
(100)/0.765*0.5	14	4.1	23	18
(010)/0.477	7.2	20	4.6[b]	2.2[b]
Observed system [8]	Hex.	Hex.	Orth.[b] + Hex.	Orth.[b] + Hex.

[a] $|\Delta| = 100 \cdot |\epsilon - \epsilon'|/\epsilon'$: Here, ϵ and ϵ' are the spacings in the child crystal and the substrate, respectively. In particular, ϵ means the intermolecular distance (or half of it) of POM in the contact plane.

[b] In the observed orthorhombic form on KI and KBr, the contact plane was assumed to be the (010) plane in Rickert and Baer [8].

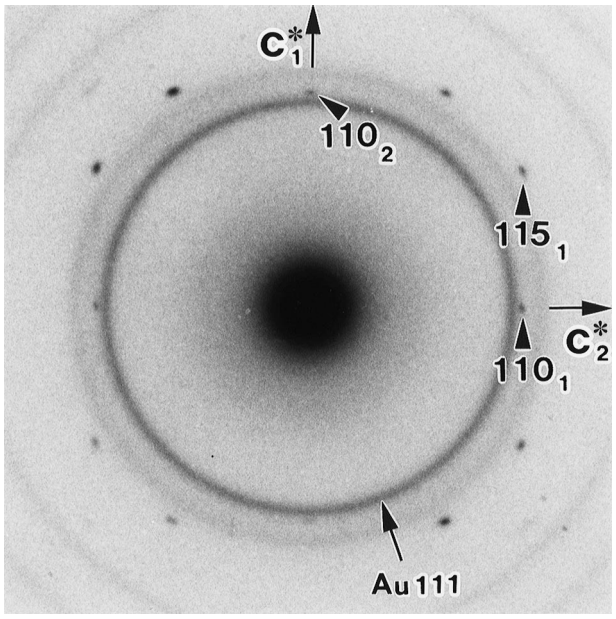

Fig. 2. SAED pattern from the rodlike crystals of POM grown isothermally on KCl in acetophenone at 125°C (contrast was reversed). The specimen was shadowed with Au and corresponds to Fig. 1b and c. The concentric rings are from Au. This pattern is the same as the one from the rodlike crystals grown on NaCl.

crystal grown on NaCl was an edge-on lamella without any conclusive experimental evidences.

As mentioned previously, we clarified the direction of chain axis in the rodlike crystal grown on NaCl by dark-field imaging together by SAED in our previous work [12]. It is, therefore, necessary to determine the direction of chain axis in the rodlike crystals grown on KCl.

3.2. Dark-field imaging

The procedure of the dark-field TEM observation was, in detail, mentioned in our previous paper [12]. Fig. 3a and b show the SAED patterns from the rodlike crystals grown epitaxially on KCl at 125°C in acetophenone: Fig. 3a was taken from the specimen without specimen tilting (equivalent to Fig. 2, but only with *C* coating) and Fig. 3b from the same specimen tilted around the c_1*-axis (viz. c_1-axis) in the microscope by 30° or − 30°. As shown in Fig. 3b, a pair of the 100 reflections (subscript 1) appears on the equator (a_1*-axis). It is noted that a pair of the 110 reflections (subscript 2) remains on the meridian in Fig. 3b. As discussed in our previous paper [12], it is difficult to take a dark-field image by using one of the four 110 reflections in Fig. 3a (without tilting), because these reflections are too weak to yield the image before the POM crystals lose their crystallinity because of electron irradiation damage. In the present work, one of the two 100 reflections in Fig. 3b, the intensity of which is much greater than that of the 110 reflection [15], was used to take the dark-field images after the specimen tilting by 30°, as in the previous work.

Fig. 4a shows the dark-field image of the rodlike crystals grown on KCl at 125°C in acetophenone, which image was

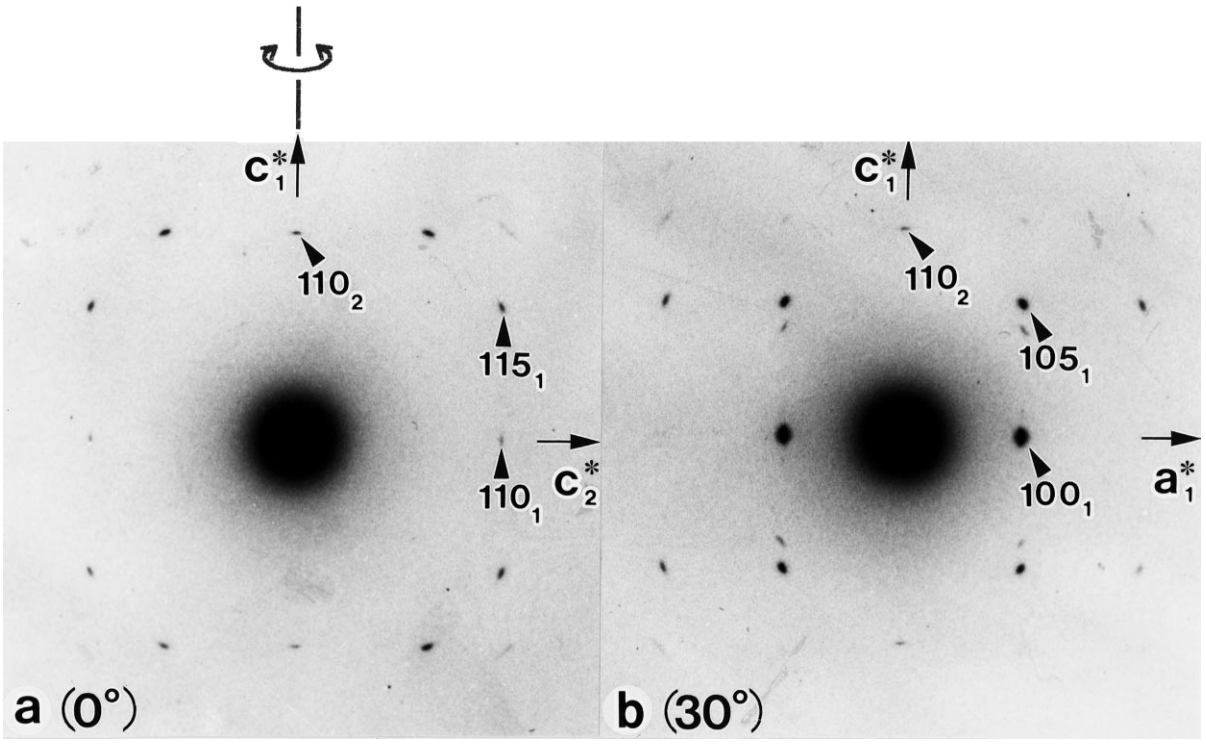

Fig. 3. SAED patterns from rodlike crystals of POM grown isothermally on KCl at 125°C in acetophenone (with no metal shadowing and reversed contrast): (a) from the untilted (0°) specimen; and (b) from the specimen tilted around the meridian by 30°. In both figures, the subscripts 1 and 2 indicate two orientations of the rodlike crystals.

obtained using the 100 reflection. The rodlike crystals appearing with much brighter contrast are orientated in the horizontal direction, similar to those on NaCl [12]. Consequently, POM molecular stems are set perpendicular to the long axis of the rodlike crystal, strictly speaking, to that of the crystalline core in the rodlike crystal. These results reveal that each of the rodlike crystals grown epitaxially on KCl is also an edge-on folded-chain lamella of POM, taking into account the lateral width of the crystals and the molecular weight of POM.

Fig. 5 illustrates our experimental scheme and result in the dark-field observation. In both Fig. 5a and b, bold bars in each rectangle represent lattice planes [the (110) or (100) plane of hexagonal POM] and the spacing between the bars accordingly means the corresponding lattice spacing. Fig. 5c represents the relationship between the cross-sectional view of the rodlike crystal of hexagonal POM and the direction of incident electron beam in TEM observation. The rodlike crystal (I) orientated in the vertical direction maintains the parallel relation between its (110) plane and the incident beam direction, in spite that the sample is untilted or tilted around the long axis of this crystal. Therefore, the 110 reflection from this crystal still remains on the meridian in the SAED pattern, even when the sample is tilted by 30° (the 110 reflection indicated with subscript 2 in Fig. 3). On the other hand, for the crystal (II) orientated in the horizontal direction, not the (110) but the (100) plane is parallel to the incident beam direction after tilting by 30°. This situation results in the appearance of the 100 reflection on the equator in the SAED pattern from this crystal (II) (Fig. 3b). As a result, in the dark-field observation using the 100 reflection on the equator the crystal (II) has much brighter contrast than the other crystal (I) (therefore, the crystal (I) is illustrated with dashed lines in Fig. 5b). From these considerations, it is concluded that the chain axis should be set perpendicular to the long axis of such a rodlike crystal, that is to say, the rodlike crystal epitaxially grown on KCl is an edge-on lamella because the (100) plane of POM is parallel to the chain axis and the axis, of course, is parallel to the substrate surface.

3.3. Internal structure of solution-grown POM crystals

Each bright striation in the dark-field image corresponds to the crystalline core of an edge-on lamella [13], which contributes to the 100 reflection in the SAED pattern (Fig. 3b) of the tilted specimen. Using the present dark-field imaging mode by TEM, we can directly estimate the crystalline-core thickness, viz. the stem length in an edge-on lamella. The method of measurement was as follows: some bright striations were randomly chosen. The mean width was measured for each striation and was regarded as the crystalline-core thickness of the corresponding lamella. When there were extremely large or too small values in the data of mean width obtained from the chosen striations, these were excluded from the data. Finally, the remaining data were averaged to obtain the average width of the striations.

Fig. 4b is a highly magnified dark-field image of the edge-on lamellae grown epitaxially on KCl at 125°C from an acetophenone solution (this image was enlarged from the same negative for Fig. 4a, but its contrast was reversed). For the specimens prepared under this condition, the average width of the bright striations (namely, of the dark ones in Fig. 4b) is estimated at 5.4 nm (± 0.7 nm). This value is obviously smaller than the average width of the rodlike crystals (9.1 nm in Fig. 1c) and also than that of the lamellar thickness (8.7 nm) [17] of the single crystals sporadically grown isothermally at 126°C from a solution in acetophenone. A similar result was already recognized on PE by our group [13].

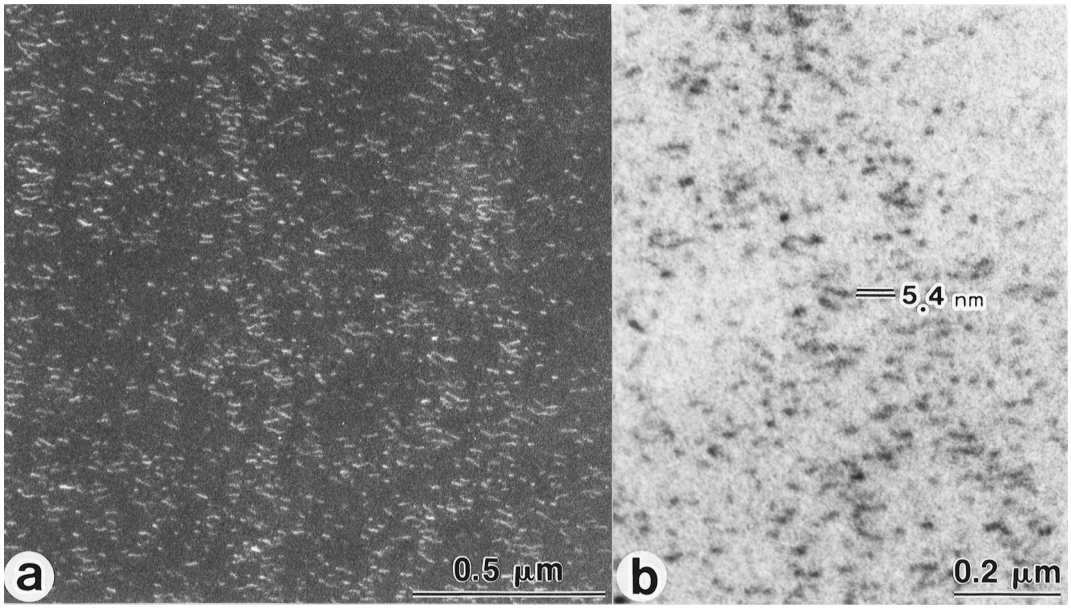

Fig. 4. (a) Dark-field image of POM rodlike crystals grown isothermally on KCl at 125°C in acetophenone. This image was taken by using the 100 reflection from the specimen tilted by 30°; and (b) highly enlarged from (a), but with reversed contrast.

Tsuji and Ihn [13] reported that one rodlike crystal of PE consisted of one or more lamellae (stacked-lamellar structure) and accordingly the width of the crystal was an integral multiple of the lamellar thickness of crystals grown from solution at the same crystallization temperature (in this connection, the true lamellar thickness of PE grown on NaCl

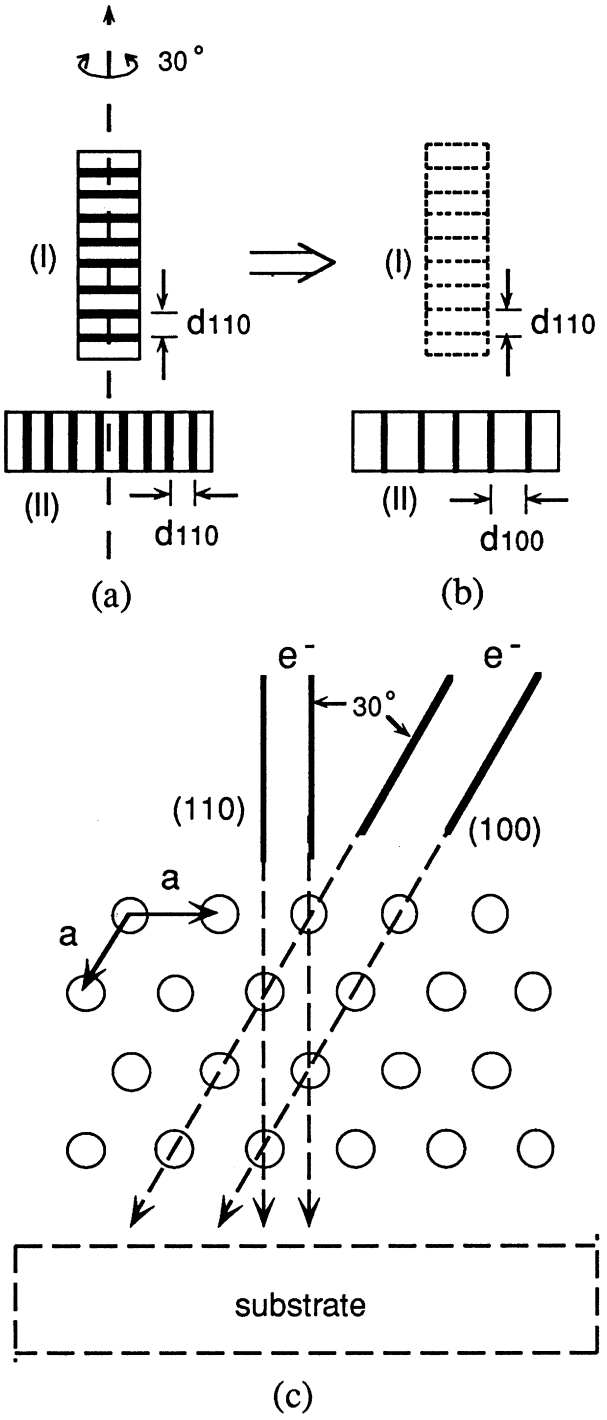

Fig. 5. (a, b) Schematic diagrams illustrating the effect of specimen tilting in the dark-field TEM observation: (a) untilted (0°); (b) tilted by 30° around the vertical axis; and (c) relationship between the cross-sectional view of hexagonal lattice of POM and the direction of the incident electron beam. Each circle (○) indicates the cross section of POM molecule.

Fig. 6. Schematic drawing for the edge-on view of the POM folded-chain lamellae. The central region represents the crystalline core and the vertical thick bars illustrate the chain stems. The shaded region represents the surface layer, which contains the fold parts of chains.

was the same as that of lamellar single crystals grown sporadically from solution at a given T_c). In this work, however, the average width of the rodlike crystals grown on KCl at 125°C from an acetophenone solution was measured at 9.1 nm (± 1.7 nm) (see Fig. 1b and c). The lamellar thickness of the single crystals sporadically grown at 126°C in acetophenone was reported to be 8.7 nm [17]. Therefore, the width of the 'isolated' rodlike crystal of POM might be regarded as the lamellar thickness of the single crystals grown at 125°C in acetophenone (see Fig. 8). It can be reasonably assumed from this fact that there is no difference between the lamellar thickness of the edge-on lamellae and that of the solution-grown single crystals if T_c and the kind of solvent are designated. The values of lamellar thickness of the single crystals grown sporadically from solution are, therefore, quoted from Korenaga et al. [17] as those of the edge-on lamellae. Based on our experimental fact that the crystalline-core thickness is smaller than the lamellar thickness, it can consequently be deduced that the edge-on crystal of POM has a surface layer containing folds on each side of the crystal (see Fig. 6), as in the edge-on crystal of PE. In the present case (acetophenone solution and T_c = 125°C), the thickness of this layer could be estimated at about 2 nm.

By another method, namely by selective degradation of the fold surface of PE single crystals with nitric acid or ozone, the existence of a 'disordered' surface layer of the

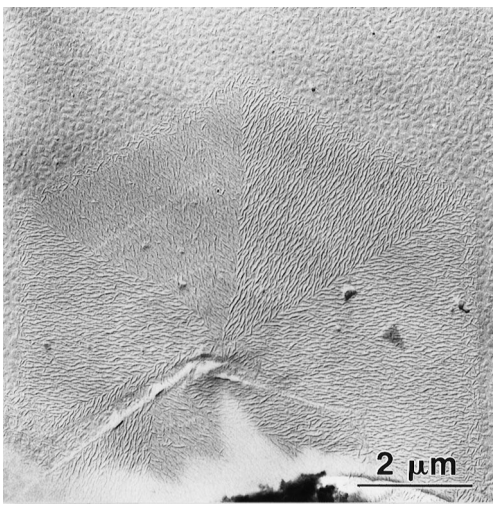

Fig. 7. POM single crystal surface-decorated with vapour-deposited PE. The single crystals were grown isothermally from an 0.1 wt% solution in *m*-cresol at 85°C. The crystallization time was 24 h.

order of a few nm in thickness was already reported [18]. According to that report, it was explained that the disordered layer was caused by the distribution of fold length, or by the positional fluctuation of folds along the stem-axis direction. We have a similar structural picture of the fold surface in PE single crystals, based on the comparative studies by TEM of PE and some cycloparaffin crystals grown from solution [13]. In the present work, unfortunately we have no conclusive model for the chain conformation or packing in the surface layer. We can, however, deduce that the structural model for the surface layer in the PE single crystal is applicable to POM, as a possible model, because the fold surface of the POM single crystal is reported to have some regularity, especially in folding direction [13], by the surface-decoration method [13,19] and by atomic force microscopy (AFM) [20], as that of the PE single crystal also does. In the present work, single crystals of the same POM sample (TENAC 5010) were grown isothermally from an 0.1 wt% solution in *m*-cresol at 85°C for 24 h. The crystallization condition was the same as that for preparation of edge-on crystals of POM, except for crystallization time and presence of substrate. The resulting single crystals were then surface-decorated with vapour-deposited PE under vacuum. Fig. 7 shows an example of the surface-decorated single crystals of POM. The deposited rodlike crystals of PE are orientated in some regular fashion over the whole surface in each sector of the POM crystal, as is similar to the results by Wittmann and Lotz [19]. This tendency might be applicable to all the POM single crystals with the hexagonal shape grown isothermally from solutions in various solvents at different T_cs. Thus, we reasonably assume that all the POM edge-on crystals prepared under the present crystallization conditions (Table 1) also have some regularity in their fold surfaces and accordingly among the possible structural models, the switch-board model may be, at least, excluded by this experimental result of surface decoration.

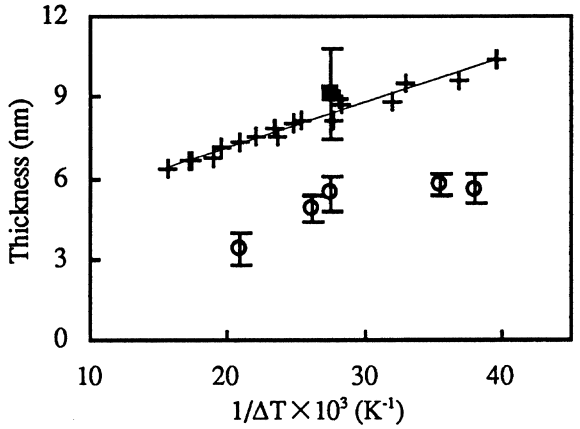

Fig. 8. Crystalline-core thickness (○) and lamellar thickness (+, ■) plotted against the inverse of the surpercooling (ΔT). The values of lamellar thickness (+), which were measured by SAXS, were quoted from Korenaga et al. [17] and that (■) was estimated by bright-field TEM observation. The vertical bars represent standard deviations.

3.4. Dependence of stem length in solution-grown POM crystals on crystallization temperature

It is well known that the lamellar thickness depends on crystallization temperature, that is to say, it increases approximately linearly with increasing inverse of the supercooling (ΔT) [21,22]. Here, ΔT is defined as $\Delta T = T_d^0 - T_c$, where T_d^0 and T_c are the equilibrium dissolution temperature for each solvent and a crystallization temperature, respectively. It is very interesting to investigate the proportion of stem length to lamellar thickness and to elucidate how the stem length (or the thickness of the surface layer) depends on crystallization temperature (or $1/\Delta T$).

For each solvent used here, T_d^0 and the lamellar thickness of POM single crystals grown at various crystallization temperatures were already measured by Korenaga et al. [17]. Though we desired to measure directly the thickness of the edge-on lamella as the width of rodlike crystals in the bright-field images, it was difficult to do so in this work except for the case shown in Fig. 1b and c. As discussed previously, the values of the lamellar thickness for various T_c were, therefore, quoted from Korenaga et al. [17]. The POM specimens examined here were prepared under the condition summarized in Table 1. For a statistical work such as the measurement of the width of bright striations in the dark-field images, KCl was better than NaCl as a substrate owing to denser nucleation (see Fig. 1).

Fig. 8 shows the $1/\Delta T$-dependence of the width of bright striations, which was obtained by the dark-field observation and also that of the lamellar thickness of single crystals grown from solution, which was estimated by small-angle X-ray scattering (SAXS) from the single crystal mat [17,22]. As can obviously be seen, the width of striations is smaller than the corresponding lamellar thickness and the width is about half the lamellar thickness at any $1/\Delta T$. Further, the width of striations increases with increasing lamellar thickness, depending on the $1/\Delta T$. Before this experiment, we had expected that the surface-layer thickness at a high $1/\Delta T$ would be smaller than that at lower $1/\Delta T$. However, Fig. 8 demonstrates that the surface-layer thickness has no tendency to decrease at higher $1/\Delta T$. The surface-layer thickness appears to be constant independently of $1/\Delta T$ or to increase with increasing $1/\Delta T$. The constant thickness leads to an interpretation that the folding manner of molecular chains during crystallization (or the resulting chain-folded structure) might be nearly identical, independent of T_c in the present system. Alternatively, if the surface-layer thickness increases with increasing $1/\Delta T$, the ratio of the surface-layer thickness to the lamellar thickness might be constant, independent of T_c. Further experiments must be carried out for final conclusion.

From only the present results, it is difficult to determine whether the crystalline-core thickness increases linearly with $1/\Delta T$ or not, though in our temperature range in Fig. 8 the lamellar thickness increases fairly linearly with increasing $1/\Delta T$ [22]. To measure more precise values of

crystalline-core thickness, lattice imaging by high-resolution TEM (HRTEM) seems to be the best. If the HRTEM images can be taken, the chain stem packing in the crystalline core and the stem length will be directly visualized. It is, however, very difficult to take an HRTEM image of the edge-on lamellae of POM, because its crystal is vulnerable to electron irradiation and in addition the orientation of its edge-on lamellae is not appropriate to HRTEM observation. Such HRTEM studies on the other polymers, which are less sensitive against electron irradiation and have adequate crystallite orientation, are advancing.

4. Concluding remarks

In the present work, the rodlike crystals of hexagonal POM were isothermally grown from dilute solution on the (001) face of NaCl or KCl at various T_c. In regard to the chain-stem orientation in the rodlike crystal, dark-field TEM imaging could directly evidence that the chain stems in the rodlike crystals are set perpendicular to the long axis of the crystals. This fact means that the rodlike crystals in question are the edge-on lamellae of POM. The dark-field image also showed that the width of the bright striation corresponding to the crystalline core in a lamella is smaller than the lamellar thickness of the single crystals measured by SAXS [17], which fact is similar to the case of PE [13,18]. For the crystals grown at any T_c, the crystalline-core thickness is, roughly speaking, 50%–60% of the corresponding lamellar thickness. The crystalline-core thickness increases with increasing lamellar thickness. Thus, the edge-on lamella of POM has a surface layer (20%–25% of the lamellar thickness) containing folds on each side of the lamella. When the lamella is tilted by 30° around the chain axis (*c*-axis), its crystalline core gives the strong 100 reflection in the SAED pattern, but, the surface layer containing folds makes a small or no contribution to the reflection possibly resulting from its ‘disorder’. The surface layer is, however, not supposed to be fully disordered as that of the switch-board model, by taking into account the results of surface decoration to the POM single crystals and of AFM [20] of them. It is, accordingly, deduced at the moment that the layer is composed, basically, of adjacent re-entrant folds, which have some fluctuation in contour length and resultant fluctuation in conformation, as in the solution-grown lamellae of PE [13].

References

[1] Mauritz KA, Baer E, Hopfinger AJ. J Polym Sci, Macromol Rev 1978;13:1.
[2] Rickert SE, Balik CM, Hopfinger AJ. Adv Colloid Interface Sci 1979;11:149.
[3] Kobayashi K, Takahashi T. Kagaku (Tokyo) 1964;34:325.
[4] Koutsky JA, Walton AG, Baer E. J Polym Sci: Part B (Polym Lett) 1967;5:177.
[5] Kiss K, Carr SH, Walton AG, Baer E. J Polym Sci: Part B (Polym Lett) 1967;5:1087.
[6] Carr SH, Keller A, Baer E. J Polym Sci: Part A-2 1970;8:1467.
[7] Mauritz KA, Hopfinger AJ. J Polym Sci: Polym Phys Ed 1975;13: 787.
[8] Rickert SE, Baer E. J Appl Phys 1976;47:4304.
[9] Balik CM, Tripathy SK, Hopfinger AJ. J Polym Sci: Polym Phys Ed 1982;20:2003.
[10] Balik CM, Tripathy SK, Hopfinger AJ. J Polym Sci: Polym Phys Ed 1982;20:2017.
[11] Sato YJ. Polym Sci: Part B: Polym Phys Ed 1990;28:1163.
[12] Fujita M, Hamada N, Tosaka M, Tsuji M, Kohjiya S. J Macromol Sci, Phys 1997;B36:681.
[13] Tsuji M, Ihn KJ. Bull Inst Chem Res, Kyoto Univ 1995;72:429.
[14] Tsuji M, Kohjiya S. Prog Polym Sci 1995;20:259.
[15] Uchida T, Tadokoro HJ. Polym Sci: Part A-2 1967;5:63.
[16] Carazzolo G, Mammi M. J Polym Sci: Part A 1963;1:965.
[17] Korenaga T, Hamada F, Nakajima A. Polym J 1972;3:21.
[18] Keller A, Martuscelli E, Priest DJ, Udagawa Y. J Polym Sci: Part A-2 1971;9:1807.
[19] Wittmann JC, Lotz B. J Polym Sci: Polym Phys Ed 1985;23:205.
[20] Nisman R, Smith P, Vancso GT. Langmuir 1994;10:1667.
[21] Hoffman JD, Davis GT, Lauritzen Jr. JI. In: Hannay NB, editor. Treatise on solid state chemistry. vol. 3, chap. 7. New York: Plenum Press, 1979:497–614.
[22] Nakajima A, Hamada F. Pure Appl Chem 1972;31:1.